

## PHENIX capabilities to probe QCD phase diagram

---

### **Kensuke Homma\*** for the PHENIX collaboration

*Hiroshima University, 1-3-1 Kagamiyama, Higashi-hiroshima, Hiroshima, Japan*

*E-mail: homma@hepl.hiroshima-u.ac.jp*

The PHENIX experiment at RHIC can provide many kinds of observables relevant for understanding of the QCD phase diagram in a coherent manner. Among many observables, we would like to focus on the measurement of the rapidity density correlation, as one of the most direct observations to define the phase boundaries which has been published recently[1]. In addition, we will summarize the PHENIX status in 2007 and present future plans on lower energy runs. The plan for the detector upgrades and possible measurements relevant for the QCD phase diagram are also presented.

*Critical Point and Onset of Deconfinement 4th International Workshop*

*July 9-13 2007*

*GSI Darmstadt, Germany*

---

\*Speaker.

## 1. Introduction

Many observations indicating the emergence of the deconfined phase have been reported from RHIC experiments[2]. However, the quantitative understanding of the QCD phase diagram is still in a premature stage even at RHIC, since those reported observations are not necessarily directly related with the phenomena characterizing critical lines or critical end-points. In order to quantify the diagram we need more simultaneous or consistent indications of characteristics directly related with phase transitions with many observables.

The PHENIX detector is suitable for such coherent observations over many different observables. Since PHENIX is primarily designed for measuring electrons and muons decayed from heavy quarks as well as the resonance states between them, we can discuss deconfined phase boundary with them. For the study of chiral phase transition, low mass vector mesons and dilepton continuum are also measurable with the good capability to identify electrons among huge hadron background. In additions to those studies, PHENIX can also provide global observables which are directly related with thermodynamic quantities, by which we can discuss phase boundaries based on the solid theoretical ground for the discussion of phase transitions. Among these observables, in the next section we would like to focus on the measurement of the rapidity density correlation, since it can be one of the most direct observations for the phase boundaries, which has been published recently[1].

In addition, we will report the PHENIX status in 2007 and a scenario in the case of lower energy runs in 2008 and 2009. Future plans for the detector upgrades and expected achievements on crucial observables are also presented.

## 2. Density correlation in longitudinal space

Growth of density fluctuations in a static medium can be a robust signature for a critical system in general. A reason why we focus on the longitudinal space rather than the transverse space is a higher possibility for the initial density fluctuations to survive in the final state, since it is expected that the expansion speed in the longitudinal space in higher energy collisions may be so fast that the evolution of the initially embedded fluctuations essentially freeze due to the rapid dilution of the medium[3]. Longitudinal space coordinate  $z$  can be transformed into rapidity coordinate  $y$  in each proper frame of sub element characterized by a formation time  $\tau$  where dominant density fluctuations are simultaneously embedded. In such a scenario,  $z$  can be directly related with  $y$  via  $dz = \tau \cos(y)dy$  and the free energy as a function of temperature  $T$  and an order parameter  $\phi$  can be expressed as

$$F(T, \phi) = \int_{\delta y} dy \int_{S_{\perp}} d^2x_{\perp} \left\{ \frac{1}{2\tau^2 \cosh(y)} \left( \frac{\partial \phi}{\partial y} \right)^2 + \cosh(y) \left( \frac{1}{2} (\nabla_{\perp} \phi)^2 + U(\phi) \right) \right\} \quad (2.1)$$

where  $\phi$  corresponds to density fluctuation amplitude around the mean density as a function of spatial points, the approximation of  $\cosh(y) \sim 1$  and  $\eta \sim y$  is valid in a narrow mid-rapidity region in high energy circumstance in Au+Au at  $\sqrt{s_{NN}} = 200\text{GeV}$ ,  $U(\phi)$  is an arbitrary potential term and degrees of freedom in the transverse plane will be integrated out in the following discussion. Since most of experimentally accessible phase spaces are relatively far from the phase boundary

or critical end-point, it is natural to use the polynomial expansion like Ginzburg-Landau for the potential term as long as order parameter  $\phi$  is very small, which is a valid assumption when the system evolves from the higher temperature side. As the potential term, we assume up to only second order term in  $\phi$  as an approximation when the system is very far from a critical temperature  $T_c$ . In such case, we expect a correlation between fluctuations in density at different points which lead to a two-point correlation function of the form of  $\alpha e^{-r/\xi} + \beta$ , where  $r$  is the one dimensional distance,  $\alpha$  is the strength of the correlation,  $\beta$  corresponds to the experimental bias independent of system temperature and  $\xi \propto (T - T_c)^{-1/2}$  is the spatial correlation length. A large increase of  $\xi$  near  $T_c$  can be a good indicator for a phase transition. In addition to  $\xi$  itself, the product  $\alpha\xi$  can also be a good indicator of a phase transition which behaves as  $(1 - T_c/T)^{-1}$ . In the GL framework, this quantity is related to the medium's susceptibility in the long wavelength limit. The details of the derivation of the relations can be found in [4] and the appendix of [1].

We present the measurement of charged particle density correlations in pseudorapidity space to search for the critical phase boundary in Au+Au collisions at  $\sqrt{s_{NN}} = 200\text{GeV}$  by the PHENIX detector[5]. The density correlation is extracted from non identified inclusive charged particle multiplicity distributions measured in magnetic field off condition as a function of pseudorapidity window size  $\delta\eta$ .

Negative Binomial Distributions (NBD) are fit to the measured multiplicity distributions, and the NBD parameters  $\mu$  (mean) and  $k^{-1}$  (deviation from a Poissonian width) are determined. The product of the correlation strength  $\alpha$  and the correlation length  $\xi$  is extracted from a known relation between the product of  $\alpha\xi$  and the NBD  $k$  parameter as a function of  $\delta\eta$ . The relation between the NBD  $k$  parameter and the pseudorapidity window size  $\delta\eta$  is known as [4][1]

$$k^{-1}(\delta\eta) = \frac{2\alpha\xi^2(\delta\eta/\xi - 1 + e^{-\delta\eta/\xi})}{\delta\eta^2} + \beta. \quad (2.2)$$

Although we have presented the preliminary results in [4] on  $\alpha$  and  $\xi$  separately, we found strong correlations between the two parameters. This was due to the smallness of  $\xi$  in HI collisions. In the limit of  $\xi \ll \delta\eta$ , which we believe holds in this measurement, Eq. (2.2) can be approximated as

$$k(\delta\eta) = \frac{1}{2\alpha\xi/\delta\eta + \beta} \quad (\xi \ll \delta\eta), \quad (2.3)$$

where experimentally we can not resolve  $\alpha$  and  $\xi$  separately, but the product  $\alpha\xi$  can be directly determined.

We expect a monotonic correspondence between initial temperature and measured energy density based on Bjorken picture [6] which in turn has a monotonic relation with the number of participant nucleons  $N_{part}$  in a collision [7]. Thus the critical behavior of  $\alpha\xi$  near  $T_c$  can be observed as a non-monotonic increase as a function of  $N_{part}$ .

As the analysis result, Fig.1 shows uncorrected charged particle multiplicity distributions in each pseudo-rapidity interval from 1/8 to 8/8 of the full rapidity coverage of  $|\eta| < 0.35$  with 0-10% events in the collision centrality. The distributions are shown as a function of the number of tracks  $n$  normalized to the mean multiplicity  $\langle n \rangle$ . The vertical error bars show the statistical errors. The solid curves were determined by performing the NBD fit. In the following analysis, we have

performed the NBD fit in each pseudo-rapidity interval size from 3/32 to 32/32 of the full rapidity coverage of 0.7 to determine a function shape in  $k$  vs.  $\delta\eta$  more precisely. The mean and RMS of reduced  $\chi^2$  values in the NBD fit over all centralities and all interval sizes used for the following analysis were obtained as 0.75 and 0.33 respectively. The mean value corresponds to typically 80% confidence level. Therefore it is good enough to assume NBD as a baseline multiplicity distribution to obtain the integrated correlation function through the  $k$  parameter based on Eq.(2.3).

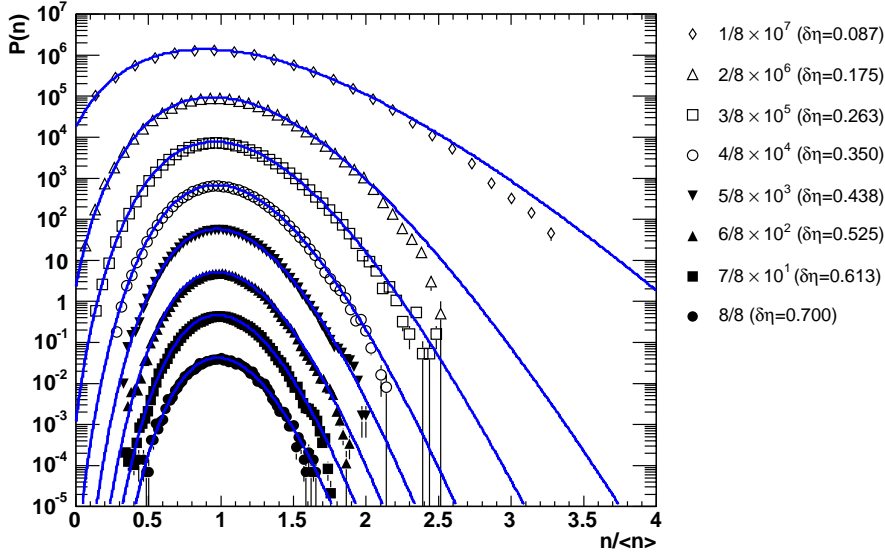
Fig.2 a) and b) show corrected  $k$  parameters as a function of pseudo-rapidity interval sizes for 10% and 5% centrality bin width cases, respectively. The centrality classes are indicated inside the figures. The vertical error bars show the quadratic sums of both statistical and systematic errors. The systematic error come from correction factors on  $k$  due to possible variations of dead or inefficient areas in the tracking detector. The solid line indicates fit results by using Eq.(2.3). The fit was performed from 0.066 to 0.7 in pseudo-rapidity. The lowest centrality bin was determined as 55-65%.

Fig.3 a) and b) show obtained fit parameters  $\beta$  and  $\alpha\xi$  as a function of the number of participants  $N_{part}$  where results for both 10% and 5% centrality bin width cases are plotted as open and filled circles respectively. The smooth solid and dotted curves are provided to guide the eye.  $N_{part}$  was obtained from the centrality classes based on the Glauber model which is explained in [8] in detail. The horizontal errors correspond to ambiguities on the mean values of  $N_{part}$  when the centralities are mapped upon  $N_{part}$ . The vertical error bars are obtained from errors on the fitting parameter by the Minit program.

A summary of the density correlation measurement is given as follows. The direct measurement of critical temperature without any tunable parameters is demonstrated by a simple differential analysis on multiplicity fluctuations, which is robust to the  $N_{part}$  fluctuations owing to the  $\beta$  parameter. The susceptibility  $\alpha\xi$  as a function of  $N_{part}$  indicates a possible non monotonic increase at  $N_{part} \sim 90$ . The corresponding Bjorken energy density is 2.4GeV/fm<sup>3</sup> with  $\tau = 1.0$  fm/c and the transverse area of 60fm<sup>2</sup>. It is interesting to note the coincidence with the energy density at which  $J/\psi$  suppression begins in NA50[9]. We need more simultaneous observations by independent measurements to conclude whether the possible non monotonic behavior is related with critical temperature or not. It is worth considering why  $\alpha\xi$  looks peak-like rather than step-like. It might suggest a rapid expansion where initially embedded fluctuations essentially freeze as expected, which would imply that relevant temperature is driven by initial stage rather than freeze-out temperature measured in the transverse plane where all evolutions are built up and the initial fluctuations tend to be wiped out.

### 3. PHENIX readiness for future runs

The goal of PHENIX runs in 2007 was the increase of statistical and systematic precision of  $J/\psi$ , jet correlations, identified hadrons in high  $p_T$ , low-mass di-electrons and so on in Au+Au collisions at  $\sqrt{s_{NN}} = 200$ GeV. Four new detector subsystems have been installed in PHENIX; a ToF subsystem (ToF-W) which can extend the capability of particle identifications in  $p_T > 8$ GeV/c, hadron blind detector(HBD) for low-mass di-electron measurements, reaction plane detector(RXNP) which can improve the reaction plane resolutions and muon piston calorimeter(MPC) which can also provide reaction plane as a part of its roles. Especially it can extend  $\eta$  measure-



**Figure 1:** Uncorrected multiplicity distributions in each  $\delta\eta$  indicated inside the figure measured in 0-10% centrality bin in Au+Au collisions at  $\sqrt{s_{NN}} = 200\text{GeV}$ . The horizontal axis is normalized by the mean multiplicities. The vertical axis is scaled by the factors indicated inside the figure.

ments of  $J/\psi$ , electrons, photons and hadrons with  $\sim 3$  times better reaction resolution compared to that reconstructed by beam-beam counter(BBC) which was only one subsystem for the reaction plane determination before 2007.

In 2008 d+Au/p+p collisions at  $\sqrt{s_{NN}} = 200\text{GeV}$  is most likely expected to get the reference data points with comparable statistical precision achieved in Au+Au runs in 2007. The lower energy runs for the understanding of the QCD phase diagram is also hoped during 2008 and 2009 before the major upgrade of the PHENIX detector. If the lower energy runs take place before 2010, RXNP takes over the role of BBC for triggering minimum bias events as well as centrality determination. However, since the timing resolution of RXNP is less accurate than BBC, good hadron identification by ToF measurements can not be achieved. Accordingly relevant observables for the phase diagram that PHENIX can provide are; global observables (multiplicity and total transverse energy,  $E_T$ ), inclusive hadron  $v_2$  with improved reaction plane resolution. The major problem related with rare probes is the available luminosity for lower energy runs in which the beam luminosity is expected to scale with  $\gamma^2 \sim 4$ , where  $\gamma$  is the Lorentz factor. Therefore, it would be difficult to provide  $J/\psi$  and low-mass di-electron results even with the help of HBD subsystem without electron cooling for the luminosity upgrade in the case of the low energy run scenario.

From around 2010 central vertex detector(VTX) will be operated which consists of two Si pixel layers and two Si strip layers with almost full azimuthal coverage and  $|\eta| < 1.2$  coverage. Since the location of RXNP and HBD interferes with VTX, those two subsystems must be taken out. Accordingly the vertex detectors take over triggering, centrality determination, reaction plane determination, and track reconstruction with large solid angle coverage.

After 2011 forward vertex detector(FVTX) will follow the VTX installation. In addition to the vertex detectors, nose cone calorimeter(NCC) which consists of electromagnetic and hadronic sectors with silicon pixel and pad readout. NCC would provide photon measurements combined

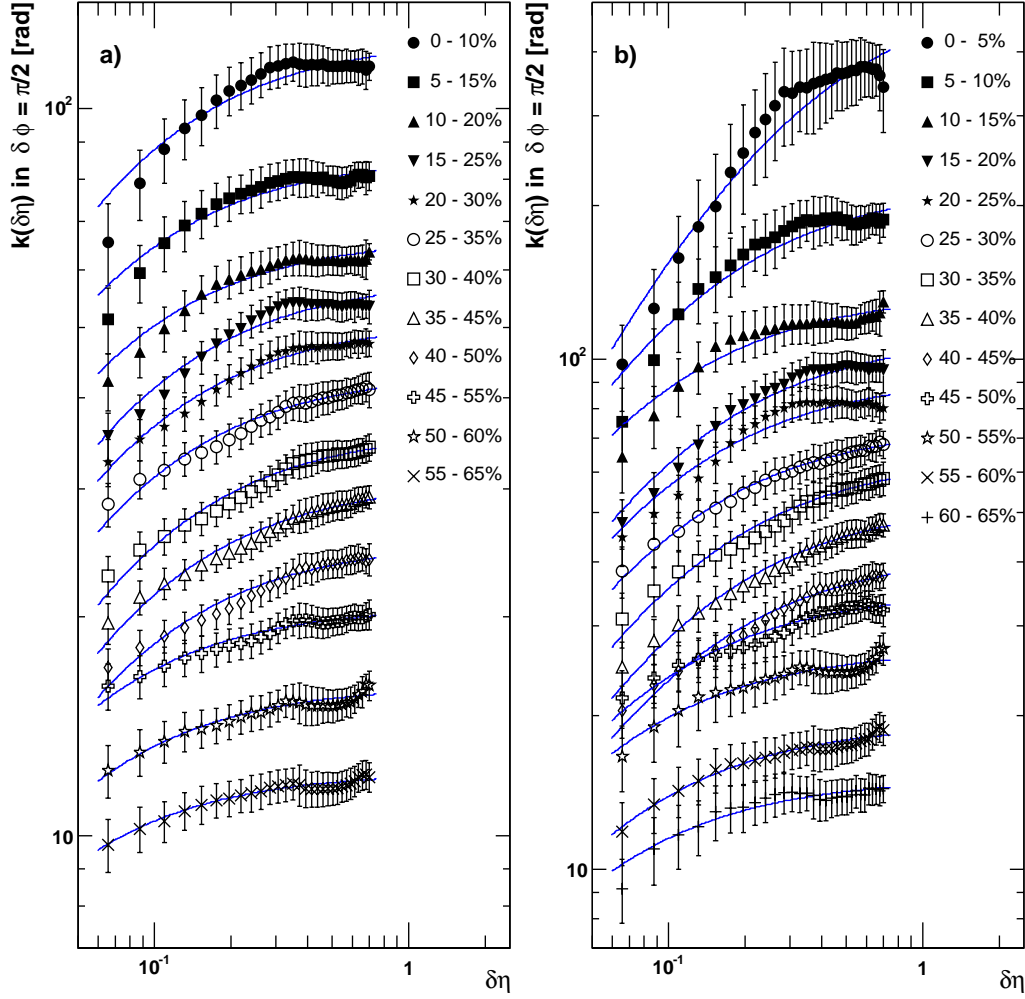


**Figure 2:** Corrected  $k$  parameters as a function of pseudo-rapidity interval sizes for centrality classes indicated inside the figure. a) and b) correspond to 10% and 5% centrality bin width cases, respectively.

with FVTX and the forward muon subsystems which enables measurement of  $\chi_c \rightarrow J/\psi + \gamma$ . After those major upgrades PHENIX can reach a full bloom on many observables coherently; multiplicity and  $E_T$  related observables with the much larger solid angle coverage,  $R_{AA}(p_T)$  of single electrons from charm and beauty decays separately,  $v_2$  of single electron from charm decay and beauty decay separately, jet tomography and  $\chi_c \rightarrow \mu^+ + \mu^- + \gamma$ .

#### 4. Summary

PHENIX can provide robust observables to probe the QCD phase diagram. For future lower energy runs, at least, PHENIX can provide basic global measurements with higher reaction plane resolutions. The biggest issue is the luminosity available for relatively rare probes such as dileptons decays in the case of lower energy run scenario. For future runs, PHENIX can provide

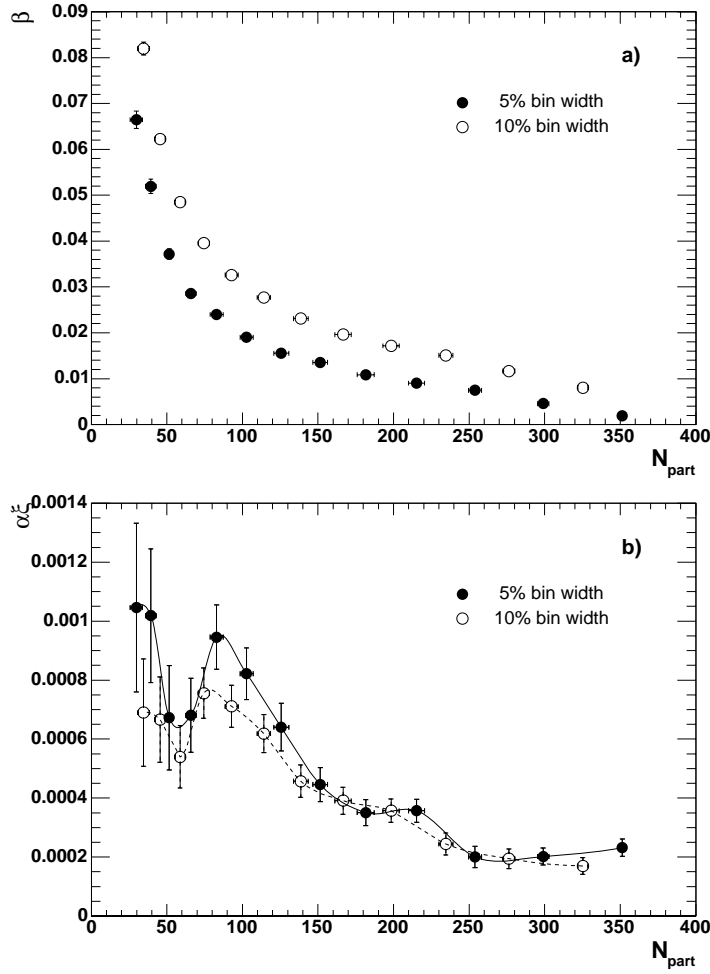


**Figure 3:** Extracted fit parameters  $\beta$  and  $\alpha\xi$  as a function of the number of participants  $N_{part}$  where results for both 10% and 5% centrality bin width cases are plotted as open and filled circles respectively. The smooth solid and dotted curves are provided to guide the eye.

more fruitful new measurements focusing on heavy quarks with the much larger solid angle in addition to measurements already established so far.

## References

- [1] S. S. Adler *et al.* [PHENIX Collaboration], arXiv:0704.2894 [nucl-ex].
- [2] K. Adcox *et al.* [PHENIX Collaboration], Nucl. Phys. A **757**, 184 (2005) [arXiv:nucl-ex/0410003].
- [3] N. Sasaki *et al.*, Europhys. Lett. **54**38-442001.
- [4] K. Homma [PHENIX Collaboration], PoS C **POD2006**, 007 (2006) [arXiv:nucl-ex/0703046].
- [5] K. Adcox *et al.* [PHENIX Collaboration], Nucl. Instrum. Meth. A **499**, 469 (2003).
- [6] J. D. Bjorken, Phys. Rev. D **27**1401983.
- [7] S. S. Adler *et al.*, PHENIX Collaboration, Phys. Rev. C **71**0349082005.

[8] S. S. Adler *et al.*, PHENIX Collaboration, Phys. Rev. C **69**0349092004.

[9] B. Alessandro *et al.* [NA50 Collaboration], Eur. Phys. J. C **39**, 335 (2005) [arXiv:hep-ex/0412036].

POS(CP0D07)053